JAAS
Journal of Analytical Atomic Spectrometry

Relative Sensitivity Factors in Glow Discharge Mass Spectrometry: the Role of Charge Transfer Ionization*

A. BOGAERTS AND R. GIJBELS

Department of Chemistry, University of Antwerp (UIA), Universiteitsplein 1, B-2610 Wilrijk-Antwerp, Belgium

A model is developed to explain the experimental relative sensitivity factors (RSF) in GDMS, based on transport and ionization of the sputtered atoms. The densities of argon metastable atoms and argon ions and the flux energy distribution of electrons throughout the discharge, which are needed to calculate the ionization factor, are obtained from explicit modelling work of the dc-GD, instead of using fitting parameters for these quantities, as was done in previous models. Since the literature contains values for cross-sections of asymmetric charge transfer ionization for only a few elements, the work was carried out in reverse order. This process was neglected in the first instance. It was found that the model based on transport and Penning ionization only (electron impact ionization is of minor importance), is not able to explain the variations in experimental RSFs for all elements. The discrepancy is clearly correlated with the (non)availability of suitable energy levels for charge transfer of the element ions. This correlation strongly suggests that ionization by asymmetric charge transfer between argon ions and the sputtered atoms is able to explain the variations in the RSF values.

Keywords: *Glow discharge mass spectrometry; relative sensitivity factor; modelling; asymmetric charge transfer*

Glow discharge mass spectrometry (GDMS) is a sensitive technique for the analysis of solid conducting materials.[1,2] One of the benefits is the fairly uniform sensitivity when determining most elements. The relative sensitivity factors (RSFs) lie generally within one order of magnitude. The RSF in GDMS is defined as the multiplication factor that has to be applied to the measured ion current ratio in order to obtain the relative concentration. For good analytical results, these RSF values have to be known accurately. This information can be obtained by analysing certified reference materials.[3,4] Empirical models have been developed to predict RSF values; they are based on fitting parameters in order to reach the best agreement between calculated and experimental values.[3–7] An overview and comparison of such models is given in ref. 8.

In the present work, a new model is presented to explain the experimental RSF values, based on the model of Vieth and Huneke[3] (*i.e.*, based on transport and ionization of the sputtered atoms). The densities and flux energy distributions of the plasma species required to calculate the ionization factor, are not considered as fitting parameters but are obtained from explicit mathematical modelling work of a dc-GD.[9–14] It will be argued that, apart from transport of sputtered atoms and from Penning ionization (electron impact ionization is of minor importance), asymmetric charge transfer between the sputtered atoms and Ar ions is mainly responsible for the variations in RSF values among different elements.

* Presented at the 1996 Winter Conference on Plasma Spectrochemistry, Fort Lauderdale, FL, USA, January 8–13, 1996.

DESCRIPTION OF THE MODEL

According to the above definition, the RSF in GDMS can be written as:

$$\frac{C_x}{C_s} = RSF\left[\frac{x}{s}\right] \times \frac{I_x}{I_s} \tag{1}$$

where I and C are the ion current and the concentration in mass units, respectively, and x and s represent the element x and the internal standard s, respectively.

This RSF value is related to the relative ion yield (RIY) in the following way:

$$RSF\left[\frac{x}{s}\right] = \frac{1}{RIY\left[\frac{x}{s}\right]} \times \frac{M_x}{M_s} \tag{2}$$

where M_x and M_s are the atomic masses.

The model presented here is partly based on that of Vieth and Huneke.[3] It states that the RIY is determined only by transport and ionization/recombination effects:

$$RIY\left[\frac{x}{s}\right] = S_T\left[\frac{x}{s}\right] \times S_I\left[\frac{x}{s}\right] \tag{3}$$

where S_T and S_I describe the transport and the ionization/recombination, respectively. The same transport factor is adapted as in the model of Vieth and Huneke, *i.e.*, transport occurs by diffusion and it is stated that elements with a higher diffusion coefficient will diffuse more quickly towards the walls, where they will be lost, so that their concentration in the plasma will be less:

$$S_T\left[\frac{x}{s}\right] = \frac{D_s}{D_x} = \frac{(r_{Ar}+r_x)^2 \times \sqrt{\mu_x}}{(r_{Ar}+r_s)^2 \times \sqrt{\mu_s}} \tag{4}$$

since $D_x \approx 1/[(r_{Ar}+r_x)^2 \times \sqrt{\mu_x}]$,[15] μ_x is the reduced mass of atoms x and Ar, and r_x is the radius of the atom x.

However, the ionization factor is treated more explicitly, based on the cross-section data of the different processes and on the densities of the plasma species, which are calculated by explicit mathematical modelling work,[9–14] instead of using fitting parameters for these quantities, which can easily take physically unrealistic values. The three ionization processes considered are Penning ionization [eqn. (5)], electron impact ionization [eqn. (6)] and asymmetric charge transfer [eqn. (7)]. Electron–ion recombination is neglected since it is generally accepted that this process is of minor importance in the GD, owing to the relatively low electron density in the plasma.[16]

$$M^0 + Ar^{m*} \rightarrow M^+ + Ar^0 + e^- \tag{5}$$

$$M^0 + e^- \rightarrow M^+ + 2e^- \tag{6}$$

$$M^0 + Ar^+ \rightarrow M^+ + Ar^0 \tag{7}$$

This yields the following equation for the RIY:

$$RIY\left[\frac{x}{s}\right] = S_I\left[\frac{x}{s}\right] \times S_T\left[\frac{x}{s}\right]$$

$$= \frac{n_{Ar^{m*}} k_{PI,x} + \sum_E j_e(E)\sigma_{EI,x}(E) + n_{Ar^+} k_{CT,x}}{n_{Ar^{m*}} k_{PI,s} + \sum_E j_e(E)\sigma_{EI,s}(E) + n_{Ar^+} k_{CT,s}} \times \frac{(r_{Ar}+r_x)^2\sqrt{\mu_x}}{(r_{Ar}+r_s)^2\sqrt{\mu_s}} \quad (8)$$

where $n_{Ar^{m*}}$, n_{Ar^+} and $j_e(E)$ are the Ar metastable density, the Ar ion density and the electron flux energy distribution, respectively; k_{PI}, k_{CT} and $\sigma_{EI}(E)$ are the Penning ionization and charge transfer rate constants and the electron impact ionization cross-section as a function of the electron energy, respectively, and r and μ are defined above.

The three ionization processes and the ways in which the Ar ion and Ar metastable densities and the electron flux energy distribution are calculated, are described below in more detail.

Penning Ionization

The cross-section of Penning ionization is taken from the literature:[17] $\sigma_{PI} \approx \sqrt{\mu} \times \pi \times R_0^3$, where R_0 is the atomic radius. The Ar metastable density throughout the discharge is calculated by a balance equation taking into account all the possible production and loss processes.[12] The production processes incorporated are: (*i*) fast electron, (*ii*) fast Ar ion impact excitation, (*iii*) fast Ar atom impact excitation and (*iv*) electron–ion radiative recombination (which is actually negligible). The loss processes include: (*i*) fast electron impact ionization and (*ii*) excitation from the metastable level to higher energy levels; (*iii*) electron quenching to the nearby resonant levels; (*iv*) metastable–metastable collisions; (*v*) Penning ionization of sputtered atoms; (*vi*) two-body and (*vii*) three-body collisions with Ar ground-state atoms; and (*viii*) diffusion and de-excitation at the walls. This results in the following differential equation, which is solved by a finite difference method (Thomas algorithm):

$$\frac{\partial n_{Ar^{m*}}}{\partial t} - D_{Ar^{m*}}\frac{\partial^2 n_{Ar^{m*}}}{\partial x^2} = r_{prod}(x) - r_{loss}(x) \quad (9)$$

where

$$r_{prod}(x) = r_{e,exc}(x) + r_{i,exc}(x) + r_{a,exc}(x) + k_{recom} n_{e_s}(x)\, n_{Ar^+}(x) \quad (10)$$

where the terms deal with formation processes (*i*)–(*iv*), respectively;

$$r_{loss}(x) = r_{ion,met}(x) + r_{exc,met}(x) + k_{quen} n_{e_s}(x)\, n_{Ar^{m*}}(x) + 2k_{met}[n_{Ar^{m*}}(x)]^2 + k_{pi} n_M(x)\, n_{Ar^{m*}}(x) + k_{2b} n_{Ar^0} n_{Ar^{m*}}(x) + k_{3b}(n_{Ar^0})^2 n_{Ar^{m*}}(x) \quad (11)$$

where the terms deal with loss processes (*i*)–(*vii*), respectively, and where $r_{e,exc}$, $r_{i,exc}$ and $r_{a,exc}$ are the electron impact, ion impact and atom impact excitation rates to the metastable level, respectively. $r_{ion,met}$ and $r_{exc,met}$ are the electron impact ionization and excitation rates from the metastable levels. k_{recom}, k_{quen}, k_{met}, k_{pi}, k_{2b} and k_{3b} are the rate constants of electron–ion recombination, electron quenching, metastable–metastable collisions, Penning ionization, two-body and three-body collisions. $D_{Ar^{m*}}$ is the diffusion coefficient of argon metastables, and n_{e_s}, n_{Ar^+}, $n_{Ar^{m*}}$, n_M, n_{Ar^0} are the densities of slow electrons, argon ions, argon metastable atoms, sputtered atoms and argon ground state atoms, respectively.

For more details about this model, see ref. 12. The resulting Ar metastable density as a function of distance from the cathode is illustrated in Fig. 1 for 100 Pa and 1000 V.

Electron Impact Ionization

The cross-section of electron impact ionization as a function of the electron energy is adapted from ref. 18. The complete electron energy distribution throughout the discharge is calculated by fast electron Monte Carlo simulations. This is the most accurate way to describe the electron behaviour. The electrons start at the cathode, created by secondary electron emission. During successive time intervals, their trajectory throughout the discharge is described by Newton's laws:

$$z = z_0 + v_{z_0}\Delta t + \frac{qE}{2m}(\Delta t)^2,\ x = x_0 + v_{x_0}\Delta t,\ y = y_0 + v_{y_0}\Delta t$$

$$v_z = v_{z_0} + \frac{qE}{m}\Delta t,\ v_x = v_{x_0},\ v_y = v_{y_0} \quad (12)$$

z, x and y and z_0, x_0 and y_0 are the positions of the electron after and before the time interval Δt; v_z, v_x and v_y and v_{z_0}, v_{x_0} and v_{y_0} are the velocities after and before the time interval Δt; $\boldsymbol{E}$ is the axial electric field; and q and m are the charge and mass of the electron.

The probability of collision (Prob) during that time interval is determined by:

$$Prob = 1 - \exp(-\Delta s \times n \times \sigma_{coll}) \quad (13)$$

where Δs is the distance travelled during Δt, n is the Ar gas density and σ_{coll} is the total collision cross-section.

This probability is compared with a random number between 0 and 1. If the probability is lower than the random number, no collision takes place and the electron is followed during the next time interval. If the probability is higher than the random number, a collision takes place. Collision processes incorporated in the model are electron impact excitation, ionization and elastic collisions. To determine which type of collision takes place, the partial collision probabilities are calculated and the total collision probability is subdivided into 10 intervals with lengths corresponding to these partial probabilities. A second random number is generated, and the interval in which this random number falls determines the type of collision that takes place. The new energy and three-dimensional direction of the electron after collision are also determined by random numbers. After this collision, the electron is followed during the next time interval, and the procedure is repeated. By following a large number of electrons in this explicit, statistical way, their behaviour can be simulated, and the electron flux energy distribution can be calculated. More details about this model can be found in refs. 9 and 11.

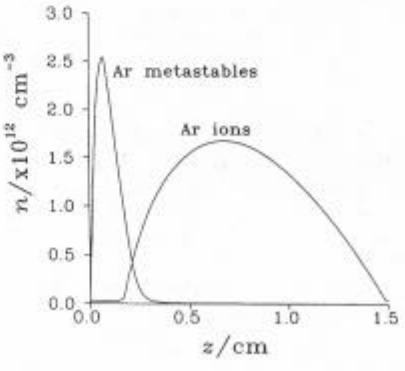

Fig. 1 Ar ion and metastable atom densities as a function of distance from the cathode at 100 Pa and 1000 V, calculated with the models in refs. 11 and 12

In Fig. 2(a) is presented the fast electron flux throughout the discharge, *i.e.*, the total flux of fast electrons scattering back and forth, calculated with the model in ref. 11, at 100 Pa and 1000 V. The flux reaches a maximum at the beginning of the negative glow owing to the back and forth scattering. In Fig. 2(b) the electron energy distribution at the anode backplate is shown. It was calculated using the model described in ref. 11 at 100 Pa and 1000 V and is representative for the energy distribution in the entire negative glow. Most of the electrons have energies too low for electron impact ionization. However, electrons of all energies are present in the plasma; a peak is even observed at maximum energy, which represents the electrons that have traversed the discharge without any collisions.

It can be shown that electron impact ionization is almost negligible compared with Penning ionization. Indeed the Penning ionization cross-section is of the order of 5×10^{-15} cm^2 corresponding to a rate constant of about 2.5×10^{-10} cm^3 s^{-1}.[17,19] Combined with the Ar metastable density of about 10^{12} cm^{-3} at 100 Pa and 1000 V (see Fig. 1),[12] this yields a rate of the order of 250 s^{-1}. The electron impact ionization cross section is of the order of 10^{-16} cm^2 at the energies of importance in the GD.[18] The electron flux is of the order of 10^{15}–10^{16} cm^{-2} s^{-1} at 100 Pa and 1000 V [see Fig. 2(a)],[11] resulting in a rate of only 0.1–1 s^{-1}. Modelling studies[12] have indeed also shown that electron impact ionization accounts for only about 1% of the total ionization of sputtered atoms at the typical discharge conditions of GDMS. Moreover, it is well known that the sputtered atoms are much more efficiently ionized than the Ar atoms, which is also due to the fact that Penning ionization is more effective than electron impact ionization.[14]

Asymmetric Charge Transfer

This process between an Ar ion and a sputtered analyte atom occurs only if the energy difference between the Ar ion ground state (or metastable level) and the energy levels of the resulting analyte ion is sufficiently small; the efficiency of this process generally decreases with growing energy difference between the levels. Charge transfer is therefore a more or less selective process. This is unlike Penning ionization which occurs unselectively for all elements having an ionization potential below the Ar metastable energy level, independently of the relative position of the energy levels.

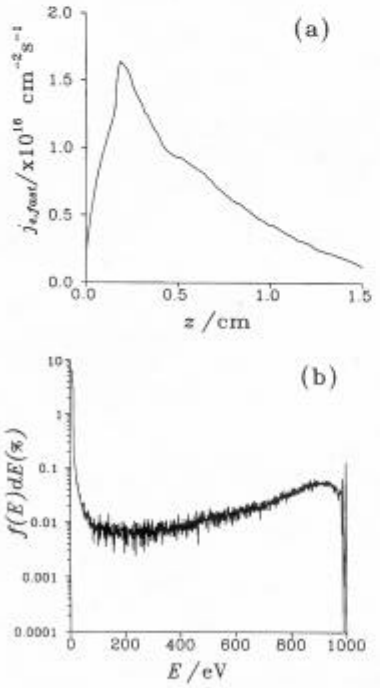

Fig. 2 Fast electron flux as a function of distance from the cathode (a) and electron energy distribution at the anode backplate (b), at 100 Pa and 1000 V, calculated using the model of ref. 11

Asymmetric charge transfer is a process that can occur over a wide range of energies, from thermal to MeV energies. The cross-section is clearly dependent on the energy of the incident particle.[20] It is generally rather small at low energies, since the electrons have time to adjust adiabatically to the changing potential as the collision proceeds and therefore the probability of a transition is small. There are of course exceptions to this behaviour owing to electron orbital promotion and to curve crossing in the temporary molecule formed in the collision.[20] The probability of charge transfer increases with increasing energy, reaches a maximum whereafter it decreases again, since at high velocities of the projectile, the time of interaction is reduced. Moreover, the electron must change its momentum in the charge-transfer process, and this is less probable at high projectile velocities.

The process of charge transfer (symmetric and asymmetric) has been studied fairly extensively both theoretically and experimentally. A good overview of the different theoretical approaches and experimental methods can be found in ref. 20. A comprehensive list of papers can be found in the literature, describing the asymmetric charge transfer process at high to very high projectile energies (several tens of eV to the MeV range), both theoretically (see for example refs. 21–34) and experimentally (see for example refs. 35–40). These studies mainly concerned the rare gases, H, C and the alkali metals. Since the discharge gas ions in the GD are more or less thermalized in the negative glow region, which constitutes the major part of the GD and the most interesting region for ionization processes, the behaviour of the asymmetric charge transfer process at thermal energies instead of the high energies treated in the above mentioned references are of specific interest in the present study. Experimental cross-sectional data of asymmetric charge transfer at thermal energies are available in the literature, but most of these data concern reactions of the rare gases and of molecular gases, such CO, H_2 and O_2 (*e.g.*, refs. 41–47). Cross-sectional data of the reaction between rare gas ions and metals are much more difficult to find in the literature, and these are just the ones of interest when using the GD as an analytical tool. A number of papers have described the asymmetric charge transfer process in a qualitative manner or shown evidence for the occurrence of such processes in GDs and ICPs (*e.g.*, refs. 48–69). Quantitative cross-sectional data, mostly obtained experimentally, are available in the literature, in connection with metal–vapour ion (hollow cathode) lasers, for specific combinations of reactants, for example He^+–Cd (*e.g.*, refs. 70 and 71), He^+–Zn (*e.g.*, ref. 72), He^+–Hg (*e.g.*, refs. 44,73–76), He^+–Cs (*e.g.*, ref. 77), Ne^+–Zn (*e.g.*, ref. 78), Ar^+–Cu (*e.g.*, ref. 79) and Xe^+–Ca,Sr (*e.g.*, ref. 80). Ref. 81 presents cross-sectional data for the different combinations of reactions between He^+, Xe^+ or Cs^+ ions with Fe, Mo, Al, Ti, Ta and C atoms, at energies ranging from 1 to 5000 eV. To our knowledge, asymmetric charge transfer cross-sectional data between Ar^+ ions and various transition element metals (Fe, Ta, Mo, ...) at thermal energies are unfortunately rarely available in the literature. It is also dangerous to deduce the cross-sections from data between other elements. Indeed, the process seems to be fairly complicated, for example, it is not always true that the smallest energy difference between energy levels yields the highest cross-section.[52,72,73] This process can only be treated adequately by

quantum mechanics, which is beyond the scope of the present paper.

Because of the virtual non-availability of these cross-sectional data, the relative importance of this process in the GD is still a controversial subject. Steers and co-workers have clearly demonstrated the occurrence of asymmetric charge transfer in the Grimm-type GD, between Ar^+ and Cu,[59,60] for Ne^+–Cu and Ne^+–Al,[61] for Ar^+–Fe[62] and between Ar^+ and Ti.[63] Recently, also Wagatsuma and Hirokawa[68] showed evidence for the occurrence of this process for Ar^+–Fe and Ne^+–Fe in a Grimm-type GD. The process has also been shown to be important in hollow cathode discharges between Ne^+ and Cu,[16,58,82] Ar^+, Ne^+ and Fe,[64] Ar^+ and Ti,[56] He^+ and Cu[53] and between Ar^+ and Cu.[79] In the early investigations of Coburn and Kay,[83] Penning ionization was considered to be the most important ionization process and charge transfer was neglected. These workers considered only charge transfer in which the ground state of the analyte ions is formed; since ΔE is then far too large, they ruled out that possibility. However, as was demonstrated by Steers and co-workers,[59–63] the resulting analyte ion can also be formed in an excited state so that ΔE can be much smaller. Levy *et al.*[84] found, on the other hand, that charge transfer between Ar^+ and Cu is unimportant in low-pressure, low-current discharges. Indeed, the Cu ions possess only one energy level, which has a good overlap with the Ar ions in the metastable state (see further, Fig. 3), and it is highly possible that the Ar ions in the metastable state have low densities in a low-pressure discharge. However, a large number of other elements do possess ionic energy levels that have a good overlap with the Ar ion ground-state level, but these elements were not investigated in ref. 84, so that the conclusions of that paper cannot be generalized. From the few cross-sectional data available (*i.e.*, for He^+–Cd[71] and He^+–Zn[72]; for these cases, a good energy overlap is found and moreover the Penning ionization and charge transfer cross-sections are measured to be of comparable magnitude) and from the Ar ion density calculated in ref. 11, it could be expected that asymmetric charge transfer can have a non-negligible role for specific elements, also in low-pressure discharges ($\approx$100 Pa).

The Ar ion density throughout the discharge is calculated with a fluid model, which is solved iteratively with the fast electron Monte Carlo model in order to obtain self-consistent results for the electric field. The relevant equations of the fluid model are the continuity equations of the Ar ions and thermalized electrons [eqns. (14) and (15), respectively), the flux equations of the Ar ions and thermalized electrons, based on diffusion and migration [eqns. (16) and (17), respectively] and the Poisson equation for the self-consistent electric field [eqn. (18)]:

$$\frac{\delta n_i}{\delta t} + \frac{\delta j_i}{\delta x} = r_i \tag{14}$$

$$\frac{\delta n_e}{\delta t} + \frac{\delta j_e}{\delta x} = r_e \tag{15}$$

$$j_i = -\mu_i n_i \frac{\delta V}{\delta x} - D_i \frac{\delta n_i}{\delta x} \tag{16}$$

$$j_e = \mu_e n_e \frac{\delta V}{\delta x} - D_e \frac{\delta n_e}{\delta x} \tag{17}$$

$$\frac{\delta^2 V}{\delta x^2} + \frac{e}{\varepsilon_0}(n_i - n_e - n_{efast}) = 0 \tag{18}$$

where the subscripts i, e and efast represent the argon ions, and thermalized and fast electrons, respectively. n, j, r, μ and D are the particle's densities, fluxes, production rates, mobilities and diffusion coefficients, respectively. V is the electrical potential. e and ε_0 are the electron charge and permittivity in a vacuum, respectively.

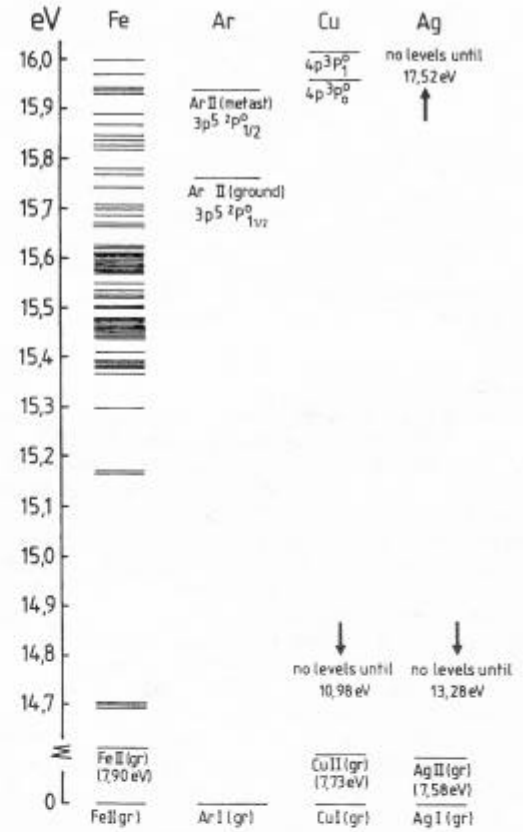

Fig. 3 Schematic representation of the energy levels of the element ions that could account for charge transfer with Ar ions, for three elements (Fe, Cu and Ag). The zero level is taken at the ground state of the atoms. Only the region of interest for charge transfer is shown (*i.e.*, 14.7–16.0 eV; the Ar II ground state and metastable levels are situated at 15.76 and 15.937 eV, respectively and it is assumed that levels lying from 1 eV below to 0.02 eV above these Ar II levels are suitable for charge transfer)

Owing to the strong coupling and severe non-linearity of these equations, solving this fluid model is a difficult numerical task. The method that was used to solve it, is based on the Scharfetter–Gummel exponential scheme. More details about this model can be found in ref. 11. The resulting Ar ion density as a function of distance from the cathode at 100 Pa and 1000 V is presented in Fig. 1. It has the same order of magnitude as the Ar metastable density, but its maximum is further into the discharge.

Since the rate constant of charge transfer is not generally known for all elements, the work was carried out in reverse order (*i.e.*, since the cross-section values are unknown, we cannot calculate the role of this process directly. Therefore, the process is in the first instance neglected, and from the discrepancy between theory and experiment the influence of the process is deduced). The RIY of the elements is calculated, taking only the transport and Penning ionization factors into account. The electron impact ionization factor can be neglected (see above). The calculated RIY is then compared with the experimental RIY and the relative difference is calculated. Moreover, by systematic investigation, the individual energy levels of all the element ions that lie close to the Ar ion ground or metastable level, and which could therefore be important for charge transfer, were sought. The relative difference between

experimental and calculated RIYs is related to these energy levels, in order to identify the actual role of charge transfer in determining the RIY.

RESULTS AND DISCUSSION

Results are presented in Table 1. The first column shows all elements incorporated in the present study. In the second column the experimental RSF values for all elements, taken from ref. 3, are presented. They were obtained with the VG9000 glow discharge mass spectrometer at 1000 V and 3 mA, which are similar discharge conditions to the ones used in the present calculations. Iron is taken as the internal standard, and therefore has an RSF value equal to 1. The experimental RIYs computed from the RSFs with eqn. (2), are given in the third column. Columns 4 and 5 represent the Penning ionization and transport factor of each element, respectively. The calculated RIY is obtained by multiplication of the Penning ionization and transport factor, and is given in the sixth column. In column 7, the relative difference between calculated and experimental RIYs is shown:

$$\Delta(\mathrm{RIY})_{\mathrm{rel}} = \frac{[(\mathrm{RIY})_{\mathrm{calc}} - (\mathrm{RIY})_{\mathrm{exp}}] \times 2}{[(\mathrm{RIY})_{\mathrm{calc}} + (\mathrm{RIY})_{\mathrm{exp}}]} \qquad (19)$$

Column 8 indicates the number of energy levels of the element ions that can possibly play a role in charge transfer with Ar ions. These were obtained by systematic investigation of the energy levels of all elemental ions under study.[85] It is not known exactly how close the energy levels must lie to each other in order to have efficient charge transfer. According to ref. 52, charge transfer can occur as long as the energy difference is less than 2 eV (the energy level of the element ion lying below the energy level of the Ar ion). Ref. 73 states that charge transfer is most effective for energy differences of 0.1–0.4 eV but that it can still take place at energy differences of 1 eV. Hence, it is not straightforward to give an exact number of the energy levels suitable for charge transfer. Therefore, in the table 'none' is written if there are certainly no levels which can play a role (*i.e.*, there are no levels lying within about 2 eV of

Table 1 Summary of the experimental RSFs and RIYs, the calculated Penning ionization [$S_{PI}(x/Fe)$] and transport [$S_T(x/Fe)$] factors and calculated RIYs, the relative differences between calculated and experimental RIYs and the number of levels suitable for asymmetric charge transfer (CT), for the different elements investigated

Element	RSF_{exp}	RIY_{exp}	$S_{PI}(x/Fe)$	$S_T(x/Fe)$	RIY_{calc}	ΔRIY_{rel}	Number of levels suitable for CT
Li	1.8	0.069	0.64	0.61	0.39	+1.40	None
Be	2.3	0.07	0.50	0.52	0.26	+1.15	None
B	1.22	0.16	0.42	0.45	0.19	+0.17	None
C	4.51	0.048	0.41	0.45	0.18	+0.74	None
N	35	0.0073	No PI	—	—	—	-
O	65	0.0044	No PI	—	—	—	-
Na	2.5	0.17	1.3	1.15	1.50	+1.60	None
Mg	1.29	0.34	1.05	0.99	1.04	+1.02	None
Al	1.39	0.35	0.94	0.91	0.86	+0.84	None
Si	1.96	0.26	0.78	0.79	0.62	+0.83	1 (far)
P	3.51	0.16	0.74	0.77	0.57	+1.13	None
S	3.34	0.17	0.74	0.77	0.57	+1.07	None
Cl	5	0.13	No PI	—	—	—	-
Ca	0.57	1.26	1.58	1.39	2.18	+0.54	Many
Ti	0.42	2.04	1.14	1.10	1.25	−0.48	Many
V	0.55	1.66	1.06	1.04	1.10	−0.40	Many
Cr	2.23	0.42	1.01	1.00	1.01	+0.83	Many
Mn	1.48	0.67	0.99	0.99	0.98	+0.38	Many
Fe	=1	=1	=1	=1	=1	0	Many
Co	1.14	0.93	1.00	1.01	1.01	+0.085	Many
Ni	1.54	0.68	1.00	1.00	1.00	+0.38	Many
Cu	4.96	0.23	1.04	1.04	1.08	+1.30	(1)
Zn	5.46	0.21	1.13	1.11	1.25	+1.42	1
Ga	4.45	0.28	1.12	1.10	1.24	+1.26	1 (far)
Ge	5.1	0.26	1.17	1.14	1.34	+1.36	1 (+1)
As	3.1	0.43	1.05	1.05	1.10	+0.87	None
Se	3.1	0.46	0.98	1.00	0.98	+0.73	None
Zr	0.64	2.55	1.42	1.34	1.90	−0.29	Many
Mo	1.3	1.32	1.23	1.20	1.48	+0.11	Many
Ru	0.93	1.95	1.18	1.16	1.37	−0.35	Many
Rh	1.39	1.33	1.20	1.18	1.41	+0.059	Many
Pd	1.87	1.02	1.22	1.20	1.46	+0.36	None
Ag	3.5	0.55	1.30	1.25	1.62	+0.98	None
Cd	9.3	0.22	1.39	1.32	1.83	+1.58	None
In	4.8	0.43	1.44	1.36	1.96	+1.28	None
Sn	2.38	0.89	1.46	1.38	2.01	+0.77	None
Sb	3.9	0.56	1.50	1.40	2.11	+1.16	None
Te	3.42	0.67	1.33	1.28	1.71	+0.88	None
W	1.46	2.25	1.34	1.30	1.75	−0.25	Many
Re	1.3	2.57	1.31	1.28	1.67	−0.43	Many
Pt	2.48	1.41	1.32	1.29	1.70	+0.19	2
Au	2.6	1.36	1.38	1.33	1.84	+0.30	1
Tl	4.9	0.75	1.70	1.56	2.65	+1.12	1
Pb	2.19	1.69	1.75	1.59	2.78	+0.49	1
Bi	4.29	0.87	1.84	1.66	3.06	+1.11	(2)

the Ar ion levels); 'many' means that a large number of energy levels are available which can account for charge transfer (*i.e.*, many levels lying within about 1 eV below and about 0.02 eV above the Ar ion levels). If there are only a few levels suitable for charge transfer, this number is mentioned in the table. When this number is in parenthesis, the level can only give charge transfer with the Ar ion metastable state, which could be less important in low pressure discharges (see above).

As an example, the energy levels of Ar ions and of ions for three elements (Fe, Cu and Ag) are shown schematically in Fig. 3. It is seen that Fe II possesses many levels suitable for charge transfer (*i.e.*, a variety of $3d^6$ 4p levels and also some $3d^64s$ and $3d^54s^2$ levels). The Cu II line has no levels lying close to the Ar II ground state and only one level showing close overlap with the Ar II metastable state (*i.e.*, the 4p $^3P^o_0$ level). The Ag II has no levels at all that could account for charge transfer.

Columns 7 and 8 show that the elements can roughly be subdivided into several groups (corresponding to two categories), according to the relative difference between calculated and experimental RIYs, and to the availability of energy levels suitable for charge transfer. It is important at this point to realize that the internal standard, Fe, is an element with many levels which allow charge transfer.

(i) For the elements Li to S, the calculated RIY is clearly higher than the experimental one [average $\Delta(\mathrm{RIY})_{\mathrm{rel}} \approx +1.0$]. Only B forms a minor exception. For N, O and Cl, the RIY is not calculated since these elements have an ionization potential higher than the Ar metastable energy and can therefore not be ionized by Penning ionization. This is clearly reflected in the low RIY and high RSF that were obtained experimentally. Moreover, the elements of this group will not undergo charge transfer with Ar, in accordance with the absence of suitable energy levels.

(ii) For the elements Ca to Ni, the experimental and calculated RIYs are more or less comparable with each other, *i.e.*, the relative difference (average value is $\approx +0.17$) is clearly smaller than for group (*i*), except for Cr. The calculated RIY is somewhat higher for the elements Ca, Cr, Mn, Co and Ni, whereas for Ti and V, the calculated RIY is slightly lower. For Fe, both experimental and calculated RIYs are by definition equal to one, and the relative difference is therefore zero. The elements of this group hence show a behaviour similar to the internal standard Fe, *i.e.*, possibility of charge transfer, as could have been expected from the energy scheme of their ions.

(iii) The elements Cu to Se again belong to the first category, since the calculated RIYs are clearly higher than the experimental ones, the relative difference being rather large ($\approx +1.2$ on average), *i.e.*, no charge transfer, in accordance with the energy levels of their ions.

(iv) The elements Zr to Rh fit into the second category (occurrence of charge transfer), with the experimental and calculated RIYs being of comparable magnitude [average $\Delta(\mathrm{RIY})_{\mathrm{rel}} \approx -0.12$]. For Mo and Rh, slightly higher calculated RIYs are obtained, while the reverse is true for Zr and Ru.

(v) The group from Pd to Te is again characterized by systematically higher calculated RIYs compared with the experimental values; $\Delta(\mathrm{RIY})_{\mathrm{rel}} \approx +1.0$ on average, *i.e.*, no charge transfer, as confirmed by the unfavourable energy levels of their ions.

(vi) For W, Re and Pt again comparable experimental and calculated RIYs are obtained [$\Delta(\mathrm{RIY})_{\mathrm{rel}} \approx -0.2$ on average]; for W and Re, the calculated RIY is lower, while for Pt the calculated value is slightly higher. These elements allow charge transfer with Ar ions, and their behaviour is similar to that of the internal standard Fe.

(vii) The last group is formed by Au to Bi, and for these elements, the calculated RIYs are again higher than the experimental values, the relative difference is $\approx +0.8$ on average, being rather small for Au and Pb, but clearly large for Tl and Bi. The ions of these elements are not likely to be formed by charge transfer with Ar ions.

Hence it appears that the systematic subdivision into different groups according to the relative difference between calculated and experimental RIYs is directly correlated with the presence or absence of ionic energy levels suitable for charge transfer with Ar ions, illustrated in column 8 of Table 1. Indeed, the elements of the groups (*i*), (*iii*), (*v*) and (*vii*) for which the calculated RIYs are too high compared with the experimental values (category 1), possess no or almost no energy levels that are suitable for charge transfer, whereas the elements of the groups (*ii*), (*iv*) and (*vi*) for which the calculated and experimental RIYs are more comparable (category 2), are characterized by a fairly large number of energy levels that can account for charge transfer. This excellent correlation strongly suggests that the occurrence or absence of charge transfer can explain the variations in the RIYs of the elements. Iron, which belongs to category 2, is taken as the internal standard. Hence for the elements of category 2, the agreement between experimental and calculated RIYs is already satisfactory, since charge transfer is compared to Fe and a so-called charge transfer factor would be of the order of 1. However, the calculated RIYs of the elements of category 1, for which charge transfer is clearly less important than for the internal standard, must be corrected by a charge transfer factor which is less than 1, in order to reach agreement with the experimental RIYs.

The fact that a few elements (*i.e.*, B, Cr and the elements in the last group) show some discrepancy in their behaviour could be due to uncertainties in the experimental RSFs or to the fact that for these elements still other effects are important. Moreover, charge transfer is a complicated process and the most suitable energy difference for charge transfer is not known. Further, it appears that the cross-section also depends on the quantum states involved. Hence it is impossible to explain exactly the variations in the relative differences among the elements within category 2. The behaviour of Cr might indicate that, in spite of the large number of levels that could on energy considerations account for charge transfer, no such excitation occurs, owing to selection rules.[62] In spite of the discrepancy for a few individual elements, which cannot be explained in detail yet, the important role of charge transfer in defining the RIY values seems highly probable.

CONCLUSION

The variations in experimental RSF and RIY were investigated, by an explicit treatment of the physical processes occurring in a dc-GD. The results strongly suggest that charge transfer is responsible for the variations in the RIYs, which could not be explained by transport phenomena and Penning ionization only.

A.B. is indebted to the Belgian National Fund for Scientific Research (NFWO) for financial support. This research is also sponsored by the Federal Services for Scientific, Technical and Cultural Affairs (DWTC/SSTC) of the Prime Minister's office through IUAP-III (conv. 49).

REFERENCES

1 Harrison, W. W., in *Inorganic Mass Spectrometry*, ed. Adams, F., Gijbels, R., and Van Grieken, R., Wiley, New York, 1988, ch. 3.
2 Marcus, R. K., *Glow Discharge Spectroscopies*, Plenum Press, New York, 1993.
3 Vieth, W., and Huneke, J. C., *Spectrochim. Acta, Part B*, 1991, **46**, 137.
4 Smithwick, R. W., III, Lynch, D. W., and Franklin, J. C., *J. Am. Soc. Mass Spectrom.*, 1993, **4**, 278.
5 Smithwick, R. W., III, *J. Am. Soc. Mass Spectrom.*, 1992, **3**, 79.

6 Ramendik G. I., Manzon, B. M., Tyurin, D. A., Benyaev, N. E., and Komleva, A. A., *Talanta*, 1987, **34**, 61.
7 Ramendik, G. I., Tyurin, D. A., and Babikov, Yu. I., *Anal. Chem.*, 1990, **62**, 2501.
8 Oksenoid, K. G., Gijbels, R., Venzago, C., and Ramendik, G. I., unpublished results.
9 Bogaerts, A., van Straaten, M., and Gijbels, R., *Spectrochim. Acta, Part B*, 1995, **50**, 179.
10 Bogaerts, A., van Straaten, M., and Gijbels, R., *J. Appl. Phys.*, 1995, **77**, 1868.
11 Bogaerts, A., Gijbels, R., and Goedheer, W. J., *J. Appl. Phys.*, 1995, **78**, 2233.
12 Bogaerts, A., and Gijbels, R., *Phys. Rev. A*, 1995, **52**, 3743.
13 Bogaerts, A., and Gijbels, R., *J. Appl. Phys.*, 1995, **78**, 6427.
14 Bogaerts, A., and Gijbels, R., *J. Appl. Phys.*, 1996, **79**, 1279.
15 Hirschfelder, J. O., Curtiss, C. F., and Bird, B. B., *Molecular Theory of Gases and Liquids*, Wiley, New York, 1964.
16 van Veldhuizen, E. M., and de Hoog, F. J., *J. Phys. D: Appl. Phys.*, 1984, **17**, 953.
17 Riseberg, L. A., Parks, W. F., and Schearer, L. D., *Phys. Rev. A, Gen. Phys. Ser. 3*, 1973, **8**, 1962.
18 Vriens, L., *Phys. Lett.*, 1964, **8**, 260.
19 Inaba, S., Goto, T., and Hattori, S., *J. Phys. Soc. Jpn.*, 1983, **52**, 1164.
20 McDaniel, E. W., Mitchell, J. B. A., and Rudd, M. E., *Atomic Collisions: Heavy Particle Projectiles*, Wiley, New York, 1993, ch. 5.
21 Rapp, D., and Francis, W. E., *J. Chem. Phys.*, 1962, **37**, 2631.
22 Olson, R. E., *Phys. Rev. A, Gen. Phys. Ser. 3*, 1972, **6**, 1822.
23 Melius, C. F., and Goddard, W. A., III, *Phys. Rev. A., Gen. Phys. Ser. 3*, 1974, **10**, 1541.
24 Ice, G. E., and Olson, R. E., *Phys. Rev. A, Gen. Phys. Ser. 3*, 1975, **11**, 111.
25 Reading, J. F., Ford, A. L., Swafford, G. L., and Fitchard, A., *Phys. Rev. A, Gen. Phys. Ser. 3*, 1979, **20**, 130.
26 Amundsen, P. A., and Jakubass, D. H., *J. Phys. B*, 1980, **13**, L467.
27 Hird, B., and Ali, S. P., *Can. J. Phys.*, 1981, **59**, 576.
28 Sidis, V., Kubach, C., and Pommier, J., *Phys. Rev. A, Gen. Phys. Ser. 3*, 1981, **23**, 119.
29 Amundsen, P. A., and Jakubassa-Amundsen, D. H., *Phys. Scr.*, 1982, **26**, 155.
30 Dube, L. J., *J. Phys. B.*, 1983, **16**, 1783.
31 Amundsen, P. A., and Jakubassa-Amundsen, D. H., *J. Phys. B*, 1984, **17**, 2671.
32 Ghosh, M., Mandal, C. R., and Mukherjee, S. C., *Phys. Rev. A*, 1987, **35**, 2815.
33 Kuang, Y. R., *J. Phys. B*, 1991, **24**, 4993.
34 Ostrovsky, V. N., *Phys. Rev. A*, 1994, **49**, 3740.
35 Peterson, J. R., and Lorets, D. C., *Phys. Rev.*, 1969, **182**, 152.
36 Perel, J., and Daley, H. L., *Phys. Rev. A, Gen. Phys. Ser. 3*, 1971, **4**, 162.
37 Sheridan, J. R., Merlo, T., and Enzweiler, J. A., *J. Geophys. Res.*, 1979, **84**, 7302.
38 Aparina, E. V., Balakai, A. A., Markin, M. I., and Tal'roze, V. L., *Dokl. Akad. Nauk SSSR*, 1983, **269**, 395.
39 Anholt, R., Stoller, Ch., Molitoris, J. D., Spooner, D. W., Morenzoni, E., Andriamorje, S. A., Meyerhof, W. E., Bowman, H., Xu, Z.-Z., Rasmussen, J. O., and Hoffman, D. H. H., *Phys. Rev. A, Gen. Phys. Ser. 3*, 1986, **33**, 2270.
40 Saito, M., Imai, M., Iwasawa, K., Sakura, N., Imanishi, N., and Fukuzawa, F., *J. Phys. Soc. Jpn*, 1992, **61**, 2748.
41 Fehsenfeld, F. C., Schmeltekopf, A. L., Goldan, P. D., Schiff, H. I., and Ferguson, E. E., *J. Chem. Phys.*, 1966, **44**, 4087.
42 Bohme, D. K., Adams, N. G., Mosesman, M., Dunkin, D. B., and Ferguson, E. E., *J. Chem. Phys.*, 1970, **52**, 5094.
43 Smith, D. L., and Futrell, J. H., *J. Chem. Phys.*, 1973, **59**, 463.
44 Johnsen, R., Leu, M. T., and Biondi, M. A., *Phys. Rev. A, Gen. Phys. Ser. 3*, 1973, **8**, 1808.
45 Johnsen, R., Macdonald, J., and Biondi, M. A., *J. Chem. Phys.*, 1978, **68**, 2991.
46 Dotan, I., Lindinger, W., and Rowe, B., *Chem. Phys. Lett.*, 1980, **72**, 67.
47 Durup-Ferguson, M., Bohringer, H., and Fahey, D. W., *J. Chem. Phys.*, 1983, **79**, 265.
48 Paschen, F., *Sber. Berl. Akad. Wiss.*, 1928, **32**, 536.
49 Berezin, I. A., *Opt. Spectrosc.*, 1969, **26**, 466.
50 Shenstone, A. G. *J. Res. Natl. Bur. Stand. Sect. A.*, 1970, **74**, 801.
51 Melius, C. F., *J. Phys. B*, 1974, **7**, 1692.
52 Green, J. M., and Webb, C. E., *J. Phys. B*, 1974, **7**, 1698.
53 Csillag, L., Janossy, M., Rozsa, K., and Salamon, T., *Phys. Lett.*, 1974, **50A**, 13.
54 Johansson, S., and Litzen, U., *J. Phys. B*, 1978, **11**, L703.
55 Littlewood, I. M., Piper, J. A., and Webb, C. E., *J. Phys. B*, 1979, **12**, 1399.
56 Danzmann, K., and Kock, M., *J. Phys. B*, 1981, **14**, 2989.
57 Barrett, J. L., Mlynczak, M. G., and Leventhal, J. J., *J. Chem. Phys.*, 1981, **75**, 2705.
58 Farnsworth, P. B., and Walters, J. P., *Spectrochim. Acta, Part B*, 1982, **37**, 773.
59 Steers, E. B. M., and Fielding, R. J., *J. Anal. At. Spectrom.*, 1987, **2**, 239.
60 Steers, E. B. M., and Leis, F., *J. Anal. At. Spectrom.*, 1989, **4**, 199.
61 Steers, E. B. M., and Leis, F., *Spectrochim. Acta*, 1991, **46B**, 527.
62 Steers, E. B. M., and Thorne, A. P., *J. Anal. At. Spectrom.*, 1993, **8**, 309.
63 Steers, E. B. M., Thorne, A. P., and Weiss, Z., presented at the *12th European Sectional Conference on the Atomic and Molecular Physics of Ionized Gases, Europhysics Conference Abstracts*, 1994, **18E**, 65.
64 Hudson, R. S., Skrumeda, L. L., and Whaling, W., *J. Quant. Spectrosc. Radiat. Transfer*, 1987, **38**, 1.
65 Farnsworth, P. B., Smith, B. W., and Omenetto, N., *Spectrochim. Acta, Part B*, 1991, **46**, 843.
66 Ogilvie, C. M., and Farnsworth, P. B., *Spectrochim. Acta, Part B*, 1992, **47**, 1389.
67 Farnsworth, P. B., and Omenetto, N., *Spectrochim. Acta, Part B*, 1993, **48**, 809.
68 Bricker, T. M., Smith, F. G., and Houk, R. S., *Spectrochim. Acta*, 1995, **50**, 1325.
69 Wagatsuma, K., and Hirokawa, K., *Spectrochim. Acta, Part B*, 1996, **51**, 349.
70 Kartazaev, V. A., and Tolmachev, Y. A., *Opt. Spectrosc.*, 1979, **45**, 620.
71 Baltayan, P., Pebay-Peyroula, J. C., and Sadeghi, N., *J. Phys. B*, 1985, **18**, 3618.
72 Baltayan, P., Pebay-Peyroula, J. C., and Sadeghi, N., *J. Phys. B*, 1986, **19**, 2695.
73 Turner-Smith, A. R., Green, J. M., and Webb, C. E., *J. Phys. B*, 1973, **6**, 114.
74 Johnsen, R., Biondi, M. A., *J. Chem. Phys.*, 1980, **73**, 5045.
75 Ostrovskii, V. N., *Sov. Phys. — JETP*, 1983, **57**, 766.
76 Belyaev, A. K., *J. Phys. B*, 1993, **26**, 3877.
77 Schuessler, H. A., Holder, C. H. Jr., and Chun-Sing, O., *Phys. Rev. A, Gen. Phys. Ser 3*, 1983, **28**, 1817.
78 Kartazaev, V. A., Piotrovskii, Y. A., and Tolmachev, Y. A., *Opt. Spectrosc.*, 1978, **44**, 362.
79 Rae, S. C., and Tobin, R. C., *J. Appl. Phys.* 1988, **64**, 1418.
80 Butterfield, K. B., Gerstenberger, D. C., Shay, T., Little, W. L., and Collins, G. J., *J. Appl. Phys.*, 1978, **49**, 3088.
81 Rutherford, J. A., and Vroom, D. A., *J. Chem. Phys.*, 1981, **74**, 434.
82 Warner, B. E., Persson, K. B., and Collins, G. J., *J. Appl. Phys.*, 1979, **50**, 5694.
83 Coburn, J. W., and Kay E., *Appl. Phys. Lett.*, 1971, **18**, 435.
84 Levy, M. K., Serxner, D., Angstadt, A. D., Smith, R. L., and Hess, K. R., *Spectrochim. Acta, Part B*, 1991, **46**, 253.
85 Moore, C. E., *Atomic Energy Levels, Volume I-III*, Nat. Stand. Ref. Data Ser., Natoinal Bureau Standards, Gaithersburg, MD, USA, 1971.

Paper 6/004051
Received January 18, 1996
Accepted April 1, 1996